



# Influence of graphene oxide on salt-polymer mud rheology and Pakistan shale swelling inhibition behavior

Shaine Mohammadali Lalji<sup>1,2</sup> · Syed Imran Ali<sup>1,2</sup> · Rqfiq Ahmed<sup>2,3</sup> · Saud Hashmi<sup>2,3</sup> · Zahoor Ul Hussain Awan<sup>2,4</sup> · Syed Wajahat Ali Qazi<sup>2,5</sup>

Received: 21 December 2021 / Accepted: 19 February 2022 / Published online: 24 March 2022  
© Saudi Society for Geosciences 2022

## Abstract

Nanoparticle adaption in comparison with micron particles reveals a relatively conducive impact on the stability of the drilling mud. Hence, the use of these particles can be a solution for the improvement of shale inhibition along with the rheological properties of water-based drilling fluid (WBDF). Salt polymer-based mud and five other samples with varying concentration of graphene oxide (GO) ranging from 0.1 to 0.5 wt% was analyzed as a shale swelling inhibitor during this study. Influence of these nanoparticles on rheological properties, filtrate volume loss, shale stability, and swelling was investigated during the experimental work. Results revealed that at different temperatures, improvement in the rheological properties of the samples was observed as the concentration of graphene oxide increases. However, at 0.5 wt%, a critical limit was observed, which indicates that further increase in the concentration of nanoparticles beyond this limit causes poor cutting carrying capacity of the mud system. Furthermore, coefficient of friction was also found to reduce at 0.4 wt% concentration. This clearly shows the formation of a slippery layer onto the interface after the addition of this particle. The results also demonstrate an improvement in shale immersion and swelling test after the addition of the GO. The sample exhibits less possibility of erosion, cracks, and disintegration after it established contact with GO mud. Additionally, an improvement in overall bulk hardness was further observed by the used of this particle. During the swelling test, it was found that the swelling characteristics of the shale sample mitigated to a great extent with the use of GO. A decrease of almost 12% in swelling was observed when the fluid system was changed from fresh water to nanoparticle mud system and change in 3% swelling, when this particle is added in the based mud system. Overall, graphene oxide proves to be a better option in improving the WBDF characteristics.

**Keywords** Graphene oxide · Bulk hardness · Swelling · Water-based drilling fluid · Lubricity

## Nomenclature

WBDF Water-base drilling fluid  
GO Graphene oxide

PHPA Partially hydrolyzed polyacrylamide  
CMC Carboxymethyl cellulose  
ROP Rate of penetration  
PAC-L Poly-anionic cellulose grade L  
SEM Scanning electron microscope

Responsible Editor: Santanu Banerjee

✉ Shaine Mohammadali Lalji  
shaine@neduet.edu.pk

Syed Imran Ali  
engrimran@neduet.edu.pk

Rqfiq Ahmed  
ahmedr@neduet.edu.pk

Saud Hashmi  
saudhashmi@neduet.edu.pk

Zahoor Ul Hussain Awan  
zahoor@cloud.neduet.edu.pk

Syed Wajahat Ali Qazi  
syedain@hotmail.com

<sup>1</sup> Department of Petroleum Engineering, NED University of Engineering & Technology, Karachi, Pakistan

<sup>2</sup> Pakistan Engineering Council (PEC), Islamabad, Pakistan

<sup>3</sup> Department of Polymer and Petrochemical Engineering, NED University of Engineering & Technology, Karachi, Pakistan

<sup>4</sup> Department of Food Engineering, NED University of Engineering & Technology, Karachi, Pakistan

<sup>5</sup> Department of Applied Chemistry & Chemical Technology, University of Karachi, Karachi, Pakistan

CEC	Cation exchange capacity
SDS	Sodium dodecyl sulphate
CoF	Coefficient of friction
CF	Correction factor
PV	Plastic viscosity
YP	Yield point
NPs	Nanoparticles
TEM	Transmission electron microscope
KCL	Potassium chloride

## Introduction

Drilling fluid is the most imperative part in the drilling industry. It is used in petroleum sector to provide various functions that includes cool and lubricate the drilling bit (Zakaria 2013), (Mortatha Al-Yasiri 2019), (Ali Esfandyari Bayata et al. 2018), (Abdo and Haneef 2011), (Hui Mao 2015), removal of drill cutting from the bottom of the hole and carry it up to the surface, maintaining the hydrostatic pressure, and help in transmission of data during well logging (Zakaria 2013), (Mortatha Al-Yasiri 2019), (Abdo and Haneef 2011), (Hui Mao 2015). Drilling fluid is primarily classified into three distinctive groups, namely, water based mud system, oil-based mud system, and synthetic based drilling fluids (Ali Esfandyari Bayata et al. 2018). As a result of environmental incompetence, the latter two mud systems are not mostly used in the oil and gas sectors (Ali Esfandyari Bayata et al. 2018), (Riley et al. 2012), (Sharma et al. 2012), (Khodja et al. 2010). Consequently, the focus is on the water based drilling fluid as these fluids are considered to be fairly inexpensive and eco-friendly (Mobeen Murtaza et al. 2020), (Aftab, et al. 2020), (Aftab et al. 2017a). Nevertheless, this mud system suffers from some shortcomings when they are been used in shale formations, as these formations have the tendency to swell and slough when comes in contact with water (Ali Esfandyari Bayata et al. 2018), (Aftab, et al. 2020), (Al-Ansari et al. 2017).

Over a past few decades, the major contemplation in the petroleum industry has been to develop a water-based drilling fluid (WBDF) drilling fluid that minimizes the wellbore instability problems, improves rheological properties, and shows high performance in drilling shale formations (Ismail et al. 2016). Sloughing of shale was preliminary tackled by the use of brine mud systems. These mud systems comprise of larger radii ions of potassium ( $K^+$ ), sodium ( $Na^+$ ), or calcium ( $Ca^{2+}$ ), which helps in developing resistance against shale swelling by reducing the swelling pressure (Khodja et al. 2010), (Oort 2003). Nevertheless, their performance fails in constraining the mud pressure penetration in the shale formation (Oort 2003). Moreover, if the concentration of these ions increases beyond a certain limit, then phase separation will also observe in the WBDF (Aftab et al. 2017a), (Chang and Leong 2014). As a result, the application of the development of polymer-based

drilling fluids was widened. These fluids help in maintaining rheological properties of drilling fluid and preventing swelling of shale formation (Aftab et al. 2017a). In the early 1990s, the use of cationic polymer was at its peak. This mud system exhibits effective cutting transportation mechanism (Gholami et al. 2018), (Fink 2015), nevertheless, wellbore stability problems and shale hydration issues were the major inadequacies for this mud (Gholami et al. 2018). This cationic mud system was then replaced with polymer-based mud having long chain, particularly, partially hydrolyzed polyacrylamide (PHPA). This chemical encapsulates the drill cutting by adhering onto the surface, thereby maintaining the size of the cutting up to the surface (Gholami et al. 2018). The encapsulation of the cutting was performed both physically and chemically (Paiva et al. 2008), (Mballa et al. 2013), (Ali et al. 2009), (He et al. 2005), which ensures the compatibility between clay mineral in shale and the polymer. Nevertheless, PHPA chemical can only be used in hard shale formation, as soft shale disintegrate easily, which consume the polymer at a rapid pace (Gholami et al. 2018), (Mballa et al. 2013). Another problem that is associated with the use of this polymer is its degradation at high thermal gradient (Hui Mao 2015), (Aftab et al. 2017a). Similar problem was encountered in the use of expensive polymers such as, carboxymethyl cellulose (CMC) and xanthan gum (Sadeghalvaad and Sabbaghi 2015). As a result, petroleum industry focuses on the development of smart drilling fluid, which has multi-functionality, stability, and is environmentally friendly in all aspects of drilling operations (Aftab et al. 2017a), (Amanullah 2009), (Zakaria and H.M., Harland G, 2012).

Formulation of smart drilling fluid is reliant upon the nanotechnology, as it unlocks a new opportunity in petroleum sector. The nanomaterials exhibit different interaction mechanism, in terms of, chemical, thermal, and mechanical properties as to those of their parent material (Aftab et al. 2017a), (Abdo and Hanneef 2013), (Amanullah and Al-Tahini 2009). Several nanoparticles (NPs) are used as an additive in drilling fluid in order to enhance the rheological properties (Aftab et al. 2017a; Aftab et al. 2017b), (Ismail et al. 2016), (Needaa Al-Malki et al. 2016), inhibiting shale swelling (Aftab et al. 2017a), (Ismail et al. 2016), (Kai Wang et al. 2020), providing wellbore stability (Kai Wang et al. 2020), (Ismail and M.S.A.R.a.B.T, 2018), (Zakaria et al. 2012), and minimizing the filtration loss (Aftab et al. 2017b), (Ismail et al., 2018). These particles are 1–100 nm in size (Zakaria et al. 2012), which combines with other additives to form an improved material having better physical and chemical properties (Alvi et al. 2018). Several studies are performed on the use of nanotechnology in oil and gas sector. The nanoparticles used in drilling operations provide an extremely high surface area to volume ratio, which significantly enhances the thermal conductivity of drilling fluid (Zakaria et al. 2012), (Amanullah et al. 2011). Moreover, NP-based fluids have higher heat transfer coefficient, which helps in dissipating heat at a faster rate on the surface,

thereby, minimizing the failure of equipment from thermal degradation (Amanullah et al. 2011). Apart from surface area to volume ratio, nanoparticles show negligible kinetic energy impact because of their nanosizes, which ultimately results in less abrasion of the downhole tools (Amanullah et al. 2011). The most important application for the use of nanoparticles is their application in the shale formation. Numerous inhibitors are developed for the inhibition process in shale, however, their performances fail up to a certain extent.

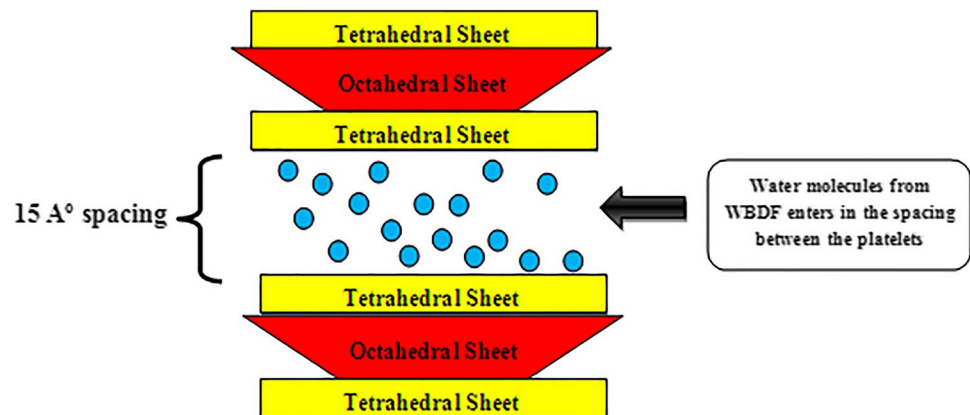
Shale is mainly classified as a clastic sedimentary rock (Gholami et al. 2018), (Díaz-Pérez et al. 2007) that mainly consists of silt, clay, and mud (Gholami et al. 2018), (Kai Wang et al. 2020), (Moslemizadeh et al. 2015), (Lalji et al. 2022; Lalji et al. 2021a; Lalji et al. 2021b). The high content of the clay mineral can be in the form of lamination (Díaz-Pérez et al. 2007), (Moslemizadeh et al. 2015), structural, or dispersed. Almost 90% of wellbore instability problems are as a result of these high clay contents (Moslemizadeh et al. 2015), (Steiger and Peter 1992). The clay minerals are electronegative in nature (Yuxiu An 2015), (Bonini et al. 2009) and are consisting of crystal platelets that are tetrahedral and octahedral in shape and are link with oxygen atoms (Moslemizadeh et al. 2015). Swelling and disintegration of clay normally arise resulting from the weak bonding between different tetrahedral sheets (Gholami et al. 2018), Van der Waals attraction, and the in situ stresses (Oort 2003). Based on the structure of these sheets and their surface charges, shale rock is classified into three distinct categories such as kaolinite, illite, and montmorillonite (Aftab et al. 2017a). Out of these three minerals, montmorillonite have the greatest tendency to swell because of the wide gap that exists between its unit as shown in Figure 1 (Aftab et al. 2017b), (Moslemizadeh et al. 2015), (Aftab, et al. 2020). No hydrogen bonding exists between the two outer tetrahedral sheets in this clay mineral. Therefore, when water molecules move into montmorillonite, the weak Van de Waals forces are unable to hold the structure of this clay mineral, which results in swelling and produces instability concerns in the wellbore (Aftab et al. 2017b).

The instability gives rises to problems such as shale sloughing, washout, caving, and finally reducing cutting carrying capacity for the drilling fluid (Saleh 2019), (Azeem Rana 2019). The swelling of shale also reduces the rate of penetration (ROP) as hydratable clay minerals are relatively soft and creates bit balling phenomena during drilling operations (Saleh 2019).

In general, there are three major mechanisms that plays vital part in the instability of a shale formation when it comes in contact with a drilling fluid (Oort 2003). Firstly, there is a rise in formation pressure as a result of drilling fluid invasion. This movement reduces the effective stresses of the formation and develops instabilities issues (Oort 2003). Secondly, increase in swelling-pressure that arises from the nonstoichiometry of the ions on the clay surface (Oort 2003), (Swai 2020). Lastly, the weakening of the bonds from the chemical alteration which reduces the effective stresses around the wellbore (Oort 2003). All these factors escalate the problems such as cutting disintegration, wellbore instability, and bit balling (Zhang et al. 2019). Hydrostatic pressure that is also known as mud pressure acts as a compressive force, which maintains the integrity of the drill cutting, however, during the transportation of the cutting up to the surface, there is a reduction in hydrostatic pressure (Oort 2003). The dropping of the mud pressure results in invasion of water molecules in the cutting, thereby, progressively taking the cutting from the dry zone to either plastic or liquid zone, where they dispersed and cause bit balling effect (Oort 2003). Apart from that, the permeability of shale is relatively on the lower side (Saleh 2019), consequently, the formation of filter cake on the face of the formation is difficult to established. To prevent all these factors, proper encapsulation of the shale is required through the formation of mud cake.

In this study, experimental work has been performed to inhibit the shale swelling using graphene oxide nanoparticles and salt polymer mud system. Changes in the rheological behavior of the conventional salt polymer mud system under study are also analyzed after the addition of nanoparticles. It was evident from the study that if this particle is used in the salt polymer mud system, then it will enhance the shale plugging behavior,

**Fig. 1** Schematic showing the structure of montmorillonite



improve the rheological properties, increase the cutting carrying capacity of the base mud, and most importantly increase the overall hardness of the shale. All these properties result in a better filtration control and wellbore stability, thus reducing the non-productive time events during drilling operations.

out under the recommended practice of API-13B-1. A total of six (06) samples were prepared as shown in Table 1, which comprises of varying concentration of NPs.

### Methodology and sampling

The method discussed in this article primarily comprises of laboratory experimentation. Figure 2 illustrates the flowchart of the experimentation carried out in this study. All the testing on the water-based drilling fluid was carried

### Formulation of water-based drilling fluid

In the laboratory, 1 barrel of mud that is equivalent to 350 cc was formulated. To prepare the base mud, 0.25 g of soda ash ( $\text{Na}_2\text{CO}_3$ ) was added in 319 mL of distilled water. After a circulation of 2 min, 18 g of potassium chloride (KCL) was added to achieve strong inhibition properties. The mixture was again agitated in Hamilton Beach Mixer for 2 min

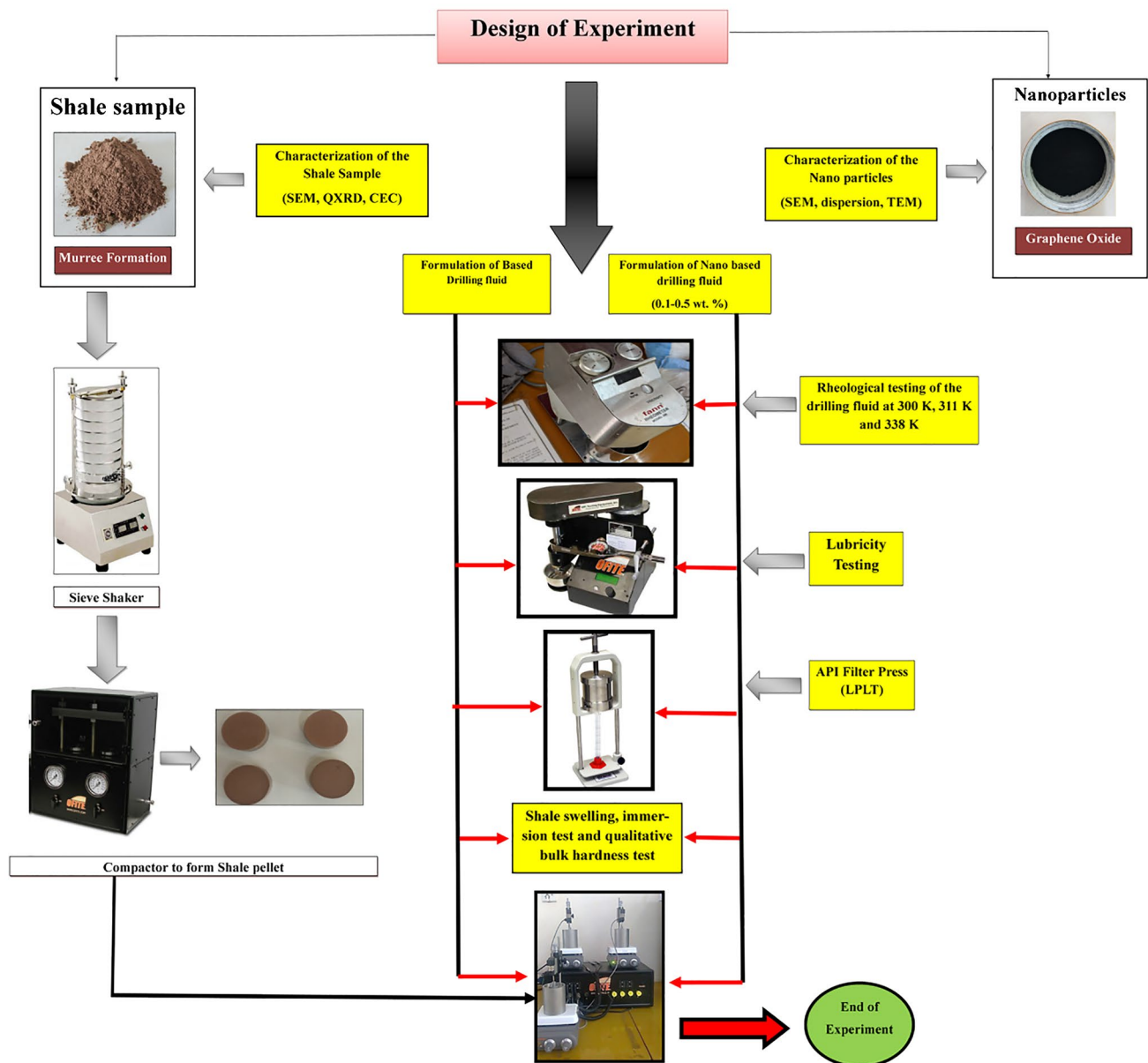


Fig. 2 Flowchart of the methodology carried out during the study

**Table 1** Sampling of the mud under investigation

Sample 1	Salt polymer mud	Base mud
Sample 2	Nanoparticle mud	Base Mud + 0.1 wt% GO
Sample 3	Nanoparticle mud	Base Mud + 0.2 wt% GO
Sample 4	Nanoparticle mud	Base Mud + 0.3 wt% GO
Sample 5	Nanoparticle mud	Base Mud + 0.4 wt% GO
Sample 6	Nanoparticle mud	Base Mud + 0.5 wt% GO

before adding 3 g of poly-anionic cellulose grade L (PAC-L). The solution was stirred 5 min before adding 0.75 g of Xanthan gum for desired rheological properties. Next,  $2 \times 10^6$  molecular weight of 0.5 g of partially hydrolyzed polyacrylamide (PHPA) was added and the solution was again mixed for 2 min for better consistency. Finally, 80 g of barite as a weighing agent was mixed in the solution with the intention of getting a mud weight of 10 ppg. This final solution was again stirred in the mixture for 30 min so as to get a better stability. During the formulation of the WBDF, API 13B-2 was followed conscientiously. For the testing of drilling mud, recommended practice of API 13B-1 was followed diligently.

### Characterization of graphene NPs and formulation of nano-based drilling fluid

Graphene oxide particles were acquired from China. Characterization of GO such as FTIR and XRD analysis are already performed in published paper (Lalji et al. 2021c). However, in this, the morphology of the purchased material was analyzed using scanning electron microscope (SEM) and transmission electron microscope (TEM). Furthermore, dispersion of GO particles in different polar protic and polar aprotic solvents was also analyzed. Moreover, the thickness of particle in this study is 5 nm.

These nanoparticles were added in base mud system after the addition of barite. The particles were added in varying concentration of 0.1–0.5 wt% (0.35–1.75 g), respectively. However, this time they were added in wet form. Before adding nanoparticles in based mud system, a solution of sodium dodecyl sulphate (SDS) and distilled water was prepared, in which GO particle powder was added in desired concentration. The dispersed solution was agitated for 30 min in a heavy duty mixture at 10,000 rpm in order to obtain a homogenous and consistent mixture of nanoparticles. This mixture was then added into the based mud, in order to formulate the nanoparticle-based drilling fluid.

To see the effect of segregation in all the mud system, it was decided to place them at room temperature for 24 h. It was observed that there were no signs of mud separation in

any of the samples, thus indicating a sound stability of the mud system.

### Murree shale formation and its characterization

Figure 2 shows the appearance of Murree shale formation that belongs to Miocene age. The sample is collected from the Hazara Kashmir Syntaxis that is situated in the northern region of Pakistan (Bossart and Ottiger 1989), (Mughal et al. 2018). The red powder color as shown in Figure 2 is resulting from the presence of hematite, which is primarily a cementing mineral (Mughal et al. 2018). Figure 3 shows the geographical location of Murree shale formation. Moreover, the morphology of the shale sample was analyzed using scanning electron microscope. This test was carried out in centralized science laboratories using JSM-6380 high performance instrument. The QXRD of the shale sample was already performed in the previous study (Lalji et al. 2021c). For the reactivity of the shale sample, cation exchange capacity (CEC) test was performed. Methylene blue solution is added to the test sample until the endpoint is reached. During this test, API RECOMMENDED PRACTICE 13B-1/ISO 10414–1 was methodically followed.

### Rheological properties

The rheological properties such as plastic viscosity (PV), yield point (YP), and gel strength (10 s, 10 min) for all the samples were measured using the Fann Rheometer Model 286. All the rheological properties were measured at three different temperatures of 300 K, 310 K, and 338 K. The Series 300 API ambient condition filter press was used to determine the filtration volume loss of all the samples. The API filter press in this study is performed at 100 psi for a standard time of 30 min (Medhi et al. 2021). During testing, API-recommended practices 13B-1 and 13B-2 were rigorously followed. For the behavior of the mud system, viscometer reading at different rpm was gathered. Figure 4 illustrates the non-Newtonian behavior of the base drilling fluid.

### Shale swelling and immersion test

For both immersion and swelling tests, shale sample was first crushed into the powder form. The powder form was then compacted in the OFITE compactor (Model 150–80–230 V) at 8000 psi for 1.5 h (Lalji et al. 2021c). Once the powder form is transformed into a pellet, it was then ready

**Fig. 3** Murree shale formation geographical location (Ali et al. 2015)

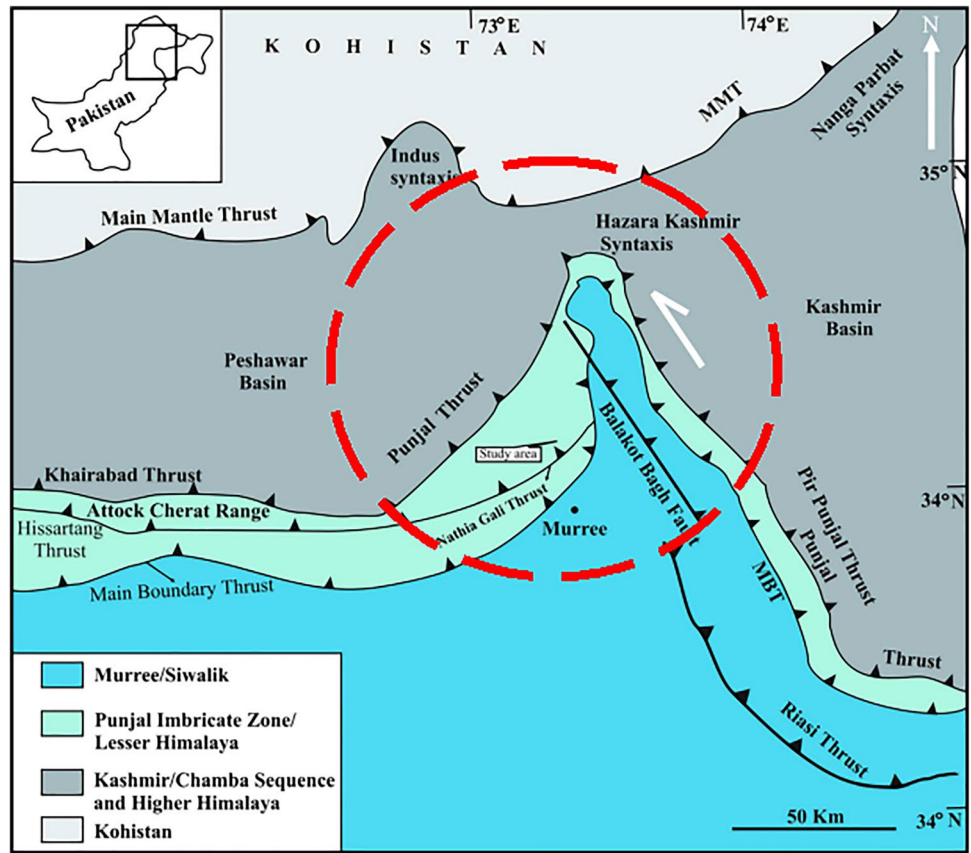
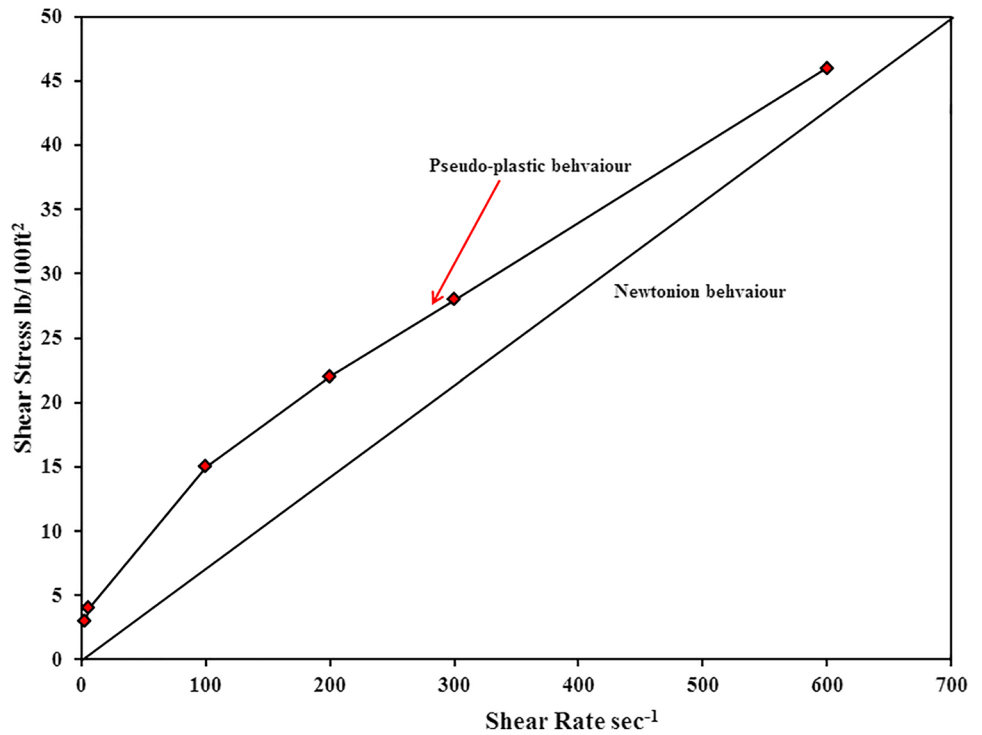


**Fig. 4** Pseudo plastic behavior of the based mud system at 300 K



for the use in the swell meter for the swelling determination. Three pellets were placed in the three different swell meter cells. These cells were already calibrated using the proper calibration procedure. Each cell comprises of 20 mL of drilling fluid (Lalji et al. 2021c) in which shale samples were placed till the steady state condition is achieved, with no further change in sample height. Cell 1 comprises of fresh water, whereas cell 2 comprises of Sample 5, while Sample 1 was in cell 3. Change in height, as recorded by the transducer, is then converted into percentage swelling, which was plotted against the experimentation time.

For the immersion test, shale pellets were immersed in Samples 1 and 5 for at least 20 h (Aftab et al. 2017b). The purpose of the test was to investigate the rock fluid interaction and stability of the sample, which will be helpful during drilling operations.

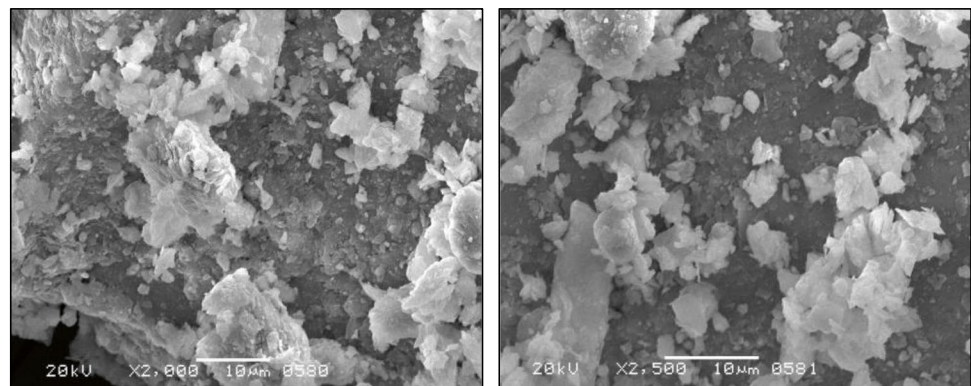
## Lubricity measurements

Lubricity of the mud was tested for 5 varying concentrations ranging from 0.1 to 0.5 wt% using the OFITE lubricity tester as shown in Figure 2. The rotating cup is first clean for 10 min with deionized water, in order to remove any impurity that exists from the previous test. The test mud samples were then placed in sample cup, and 150 inch-pound of torque is applied to the test sample to measure the coefficient of friction (CoF)  $\mu$ . Equations 1 and 2 were used to determine the lubricity coefficient (Aftab et al. 2017).

$$\text{Correction Factor (CF)} = \frac{34}{\text{Av. Reading}} \quad (1)$$

$$\text{Lubricity Coefficient} = \frac{\text{Meter Reading} * \text{CF}}{100} \quad (2)$$

**Fig. 5** SEM analysis of shale sample



## Qualitative hardness test

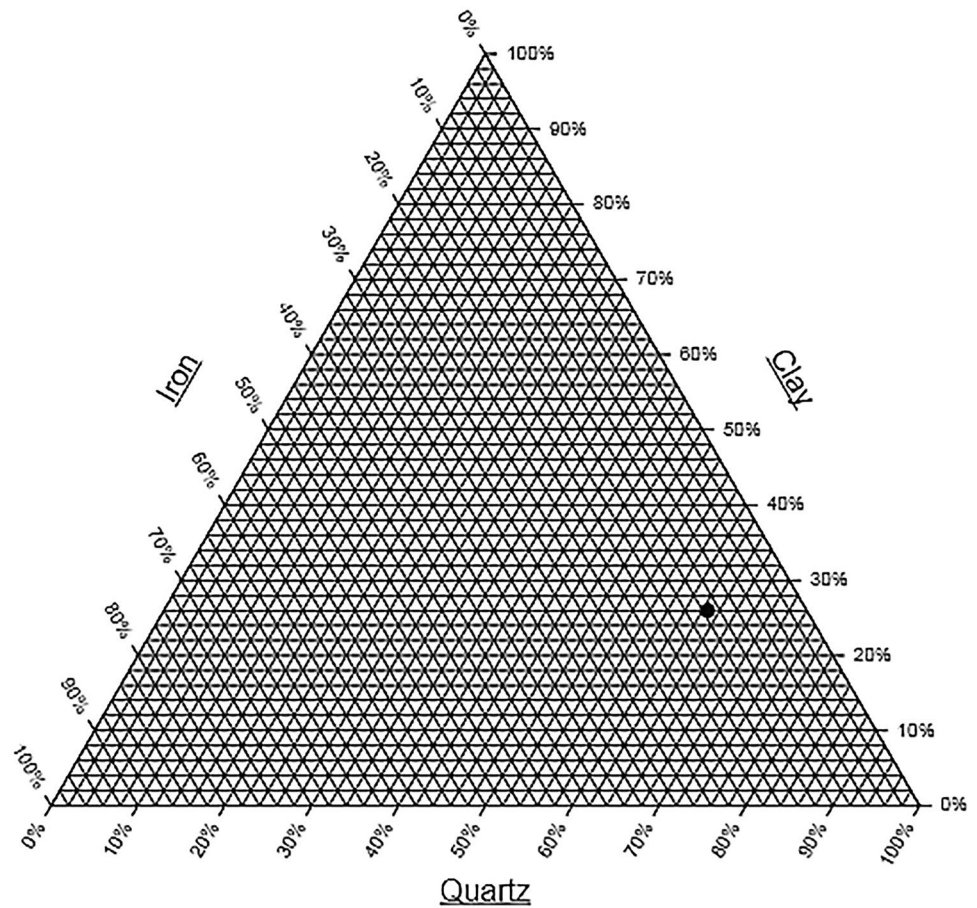
The qualitative hardness test was conducted on the sample after the rock fluid interaction. The purpose of this test was to measure the force required to disintegrate the sample after it has been exposed to mud system. The samples were exposed to different masses ranging from 3 to 15 kg. The masses were gradually increased until the sample starts to crack. The total mass required to break the shale sample was then recorded.

## Results and discussion

### Characterization of shale sample

Scanning electron microscope (SEM), both instinctively and quantitatively, provides the information related to shale pore size and its morphology. Figure 5 shows the SEM image of the shale sample. Irregularities can be observed on the surface of the shale sample. Apart for that, undulations can also be witnessed, thus signifying the crystalline type of structure on its surface. Moreover, because of montmorillonite, there is significant stacking of sheet that exists in the material (Sengupta et al. 2008). Another reflection that can be made from Figure 5 is the presence of large number of micropores, which ultimately results in a large surface area of this formation. The mineral found in this shale formation are mostly quartz, smectite, diopside, kaolinite, illite, pyrite, hematite, and magnetite (Mughal et al. 2018). Figure 6 indicates the ternary plot for the sample of shale developed from QXRD result. This ternary plot indicates 62% of quartz, 26% of clay, and remaining 12% of iron mineral. A total of 62% of the quartz indicates that the sample of shale is highly siliceous (Mughal et al. 2018). The presence of iron minerals are indication of the weathering and deposition of hydrothermal veins in the shale sample (Mughal et al. 2018). Exactly 26% of the clay minerals that exist within this formation are

**Fig. 6** Ternary plot develop from QXRD result showing the mineral composition of the shale formation



because of the weathering of the primary minerals (Mughal et al. 2018).

Once the QXRD of the sample was performed, the shale sample was then tested for its cation exchange capacity (CEC). It was experimentally investigated that the sample of shale has the CEC of  $17 \frac{\text{meq}}{100\text{gm}}$ . This value indicates a very high percentage of exchangeable ions on the surface of the clay mineral. Out of 26% of the clay mineral, 13.6% is a hydratable clay mineral smectite that is also known as montmorillonite. This mineral has the largest surface area of around  $700\text{--}800 \text{ m}^2/\text{g}$  (Khan, et al. 2020) and comprises of large proportion of exchangeable ions on its surface. Moreover, illite has a surface area in range of  $100\text{--}200 \text{ m}^2/\text{g}$ , which is also utterly responsible for this high CEC value (Khan, et al. 2020) in this shale formation.

### Characterization of graphene oxide

Figure 7 shows the scanning electron microscope (SEM) analysis of graphene oxide. The image clearly demonstrates the wrinkled characteristics morphology of the sample. It further appears that different random sheets with distinct boundaries are combined together to form these wrinkled

surface. Moreover, it is visible that exfoliation and folding of graphene oxide results from these crumpled surfaces.

Furthermore, as shown in Figure 8, the dispersion effect of GO was analyzed in three different solvents. GO was dissolve in solvents such as polar protic solution of deionized water and 1-propanol and a polar aprotic solution of acetone with 45 min sonication to see the dispersion effect (Ravi Kumar 2019). It was observed that after 45 min, a colloidal suspension was obtained in deionized water. On the contrary, acetone and 1-propanol show poor dispersion effect of GO (Johnson and Karl 2015). Both the solvents demonstrate segregation of GO at the bottom of the test tube. It was further noticed that after the period of 3 days, all the three liquids show a formation of clear solvent and the settling of GO at the bottom, which indicates poor dispersibility of GO in these solvents.

Moreover, the structural characterization of graphene oxide was performed through transmission electron microscope (TEM) imaging as shown in Figure 9. The dark areas in the figure indicate the stacking of several nanolayering of graphene oxide. On the other hand, the area with higher transparency indicates the stacking of few layers of graphene oxide nanostructure exfoliation.



**Fig. 7** SEM analysis of graphene nanoplatelet obtained from China-based company

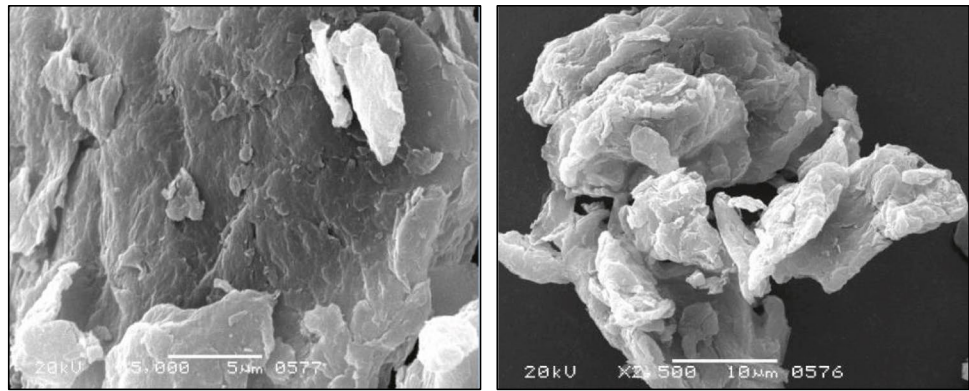


**Fig. 8** Dispersion effect of graphene oxide in different solvent **a** after sonication, **b** 45 min, and **c** 3 days after sonication

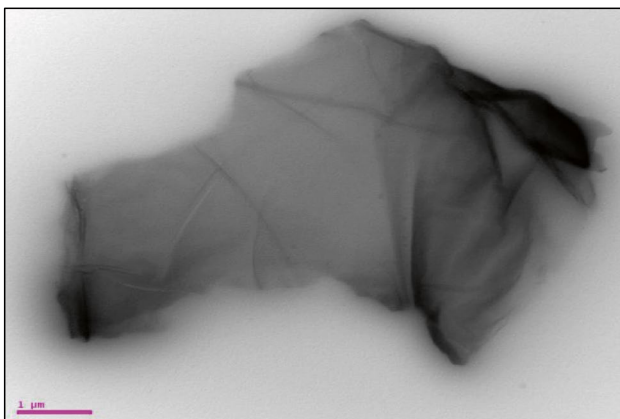
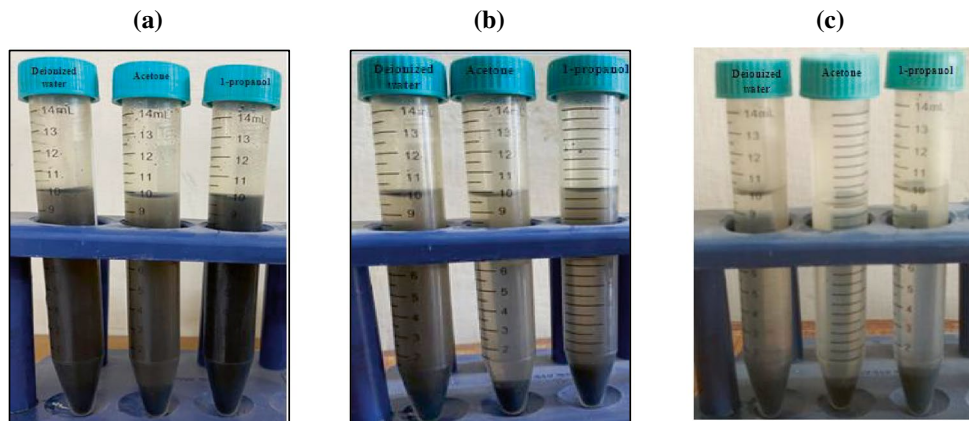


**Fig. 9** TEM images of graphene oxide

### Rheogram of nanoparticle-based drilling fluid at different temperature

Figure 10 shows the Rheogram of water based drilling fluid having varying concentrations of nanoparticles are three different temperatures. All the plots indicate the shear thinning

behavior at all temperatures. This pseudo plastic nature of the drilling fluid clear indicates towards the gel network that GO form inside the drilling mud. It was further evident from Fig. 10a–e that an increase in temperature causes a reduction in shear stress of the drilling fluid (Wang et al. 2012), (Zhao et al. 2008). Additionally, increasing the concentration of NPs in the mud system causes an increase in shear stress of the drilling fluid (Ahmed et al. 2020).

The flow behavior of the mud system at all three temperatures follows non-Newtonian pattern. Hence, the shear stress versus shear rate is best tailored with Power law model. Furthermore, Figure 11 shows the graphically representation of the consistency index and fluid flow index of the drilling fluid at varying temperature and concentration of NPs. It is apparent from Figure 11a that increase in weight percentage of NPs in the base mud causes an increase in fluid consistency index (Messaudi et al. 2018). This parameter further reveals the thickness of the mud that is form during drilling operations. Moreover, fluid flow index is shown in Figure 11b. For shear thinning behavior of the drilling fluid, this index is less than 1 (Messaudi et al. 2018). It was observed that for all concentrations of GO, this parameters remain below 1,

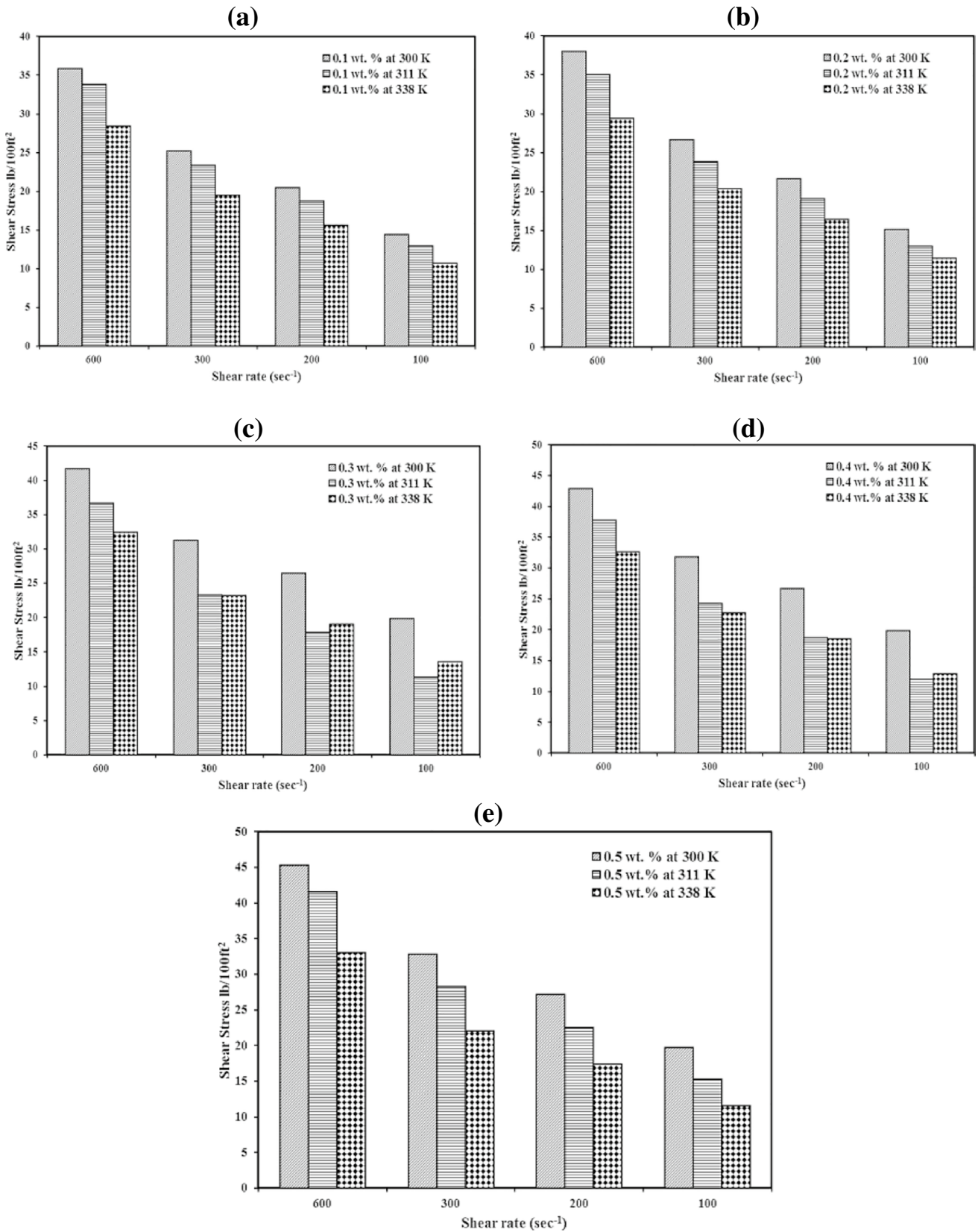


**Fig. 10** a–e (0.1–0.5 wt%) Rheogram of nanoparticle-based drilling fluid at different concentrations (Extreme left column for 300 K, middle column for 311 K and right column for 338 K at each shear rate).

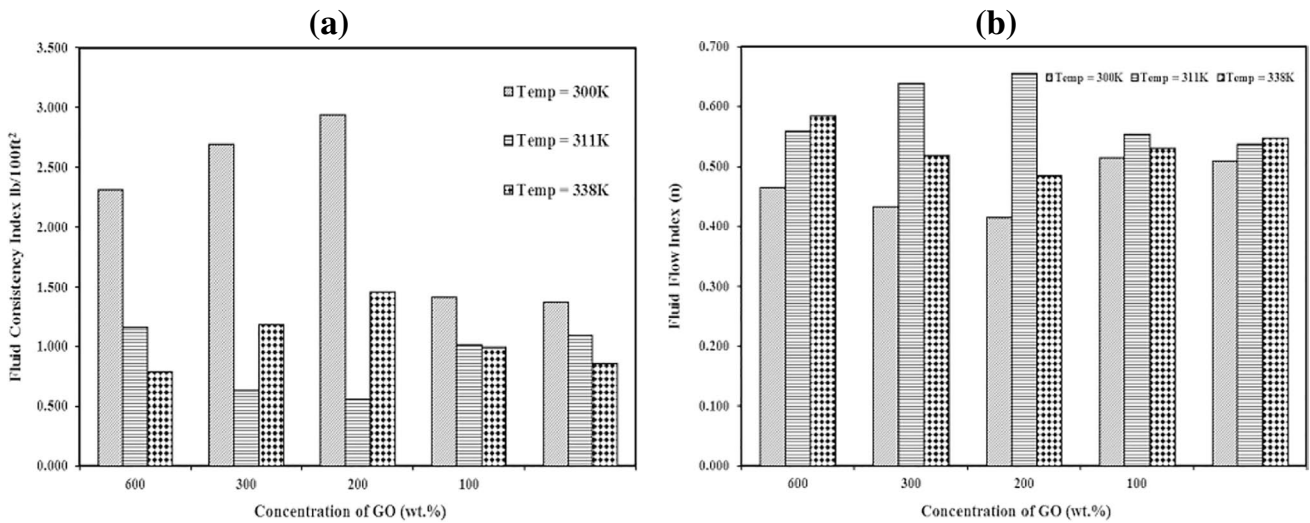


Fig. 11 Power law model parameters: **a** consistency index; **b** fluid flow index

which proves that this fluid does not loses its shear thinning ability at all temperatures and concentration of GO.

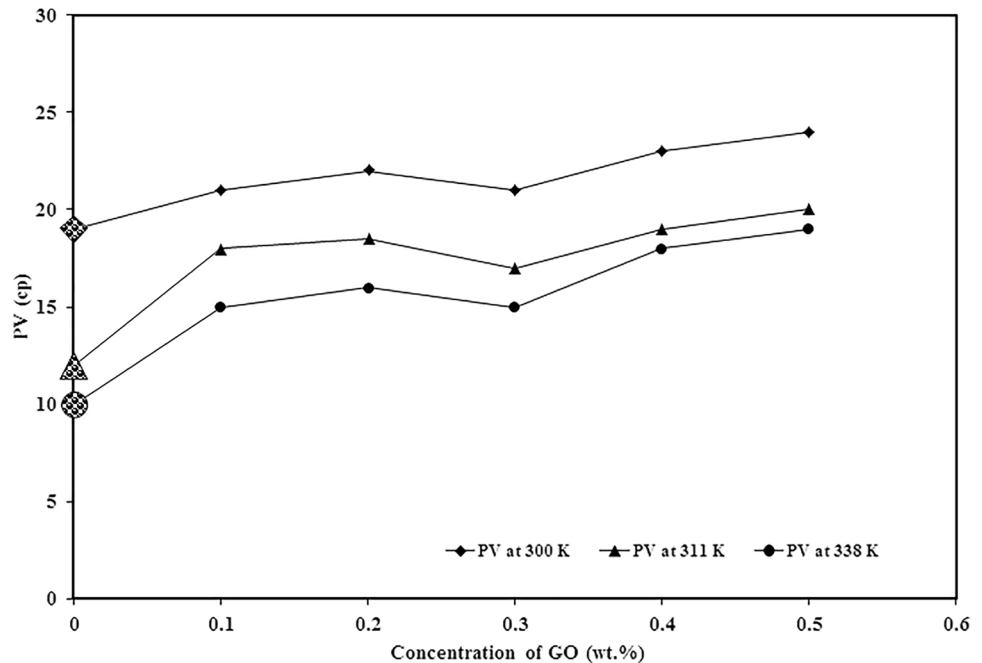
### Rheological properties and filtration test of drilling fluid

#### Effect of particle concentration and temperature on plastic viscosity

Figure 12 illustrates the effect of changing the temperatures on the plastic viscosity of nanoparticles mud system.

Generally, a higher value of PV for a drilling fluid will cause an increase in pumping rate for that fluid (Ali Esfandyari Bayata et al. 2018), (Lalji et al. 2021c), (Aramendiz and Imqam 2020). This property also describes the mechanical interaction that develops between the particles in the drilling fluid (Aramendiz and Imqam 2020). It was observed that as the temperature increases, PV decreases (Aramendiz and Imqam 2020). Furthermore, it is apparent that increase in concentration of nanoparticles shows an increase in PV (Ahmed et al. 2020). This is because of the increase in total dispersed concentration of the solid particles in the mud system. Moreover, plastic viscosity was improved with the

Fig. 12 Effect of temperatures along with nanoparticle concentrations on PV



addition of GO. It was experimental investigated that at 300 K, 311 K, and 338 K, the base mud had a plastic viscosity of 19, 12, and 10 cP, respectively. However, at all three temperatures, PV values were increased that signifies the improvements in PV by using GO. It may be owing to resistance that develops by GO and the liquid medium of the drilling fluid (Aftab et al. 2017b). It is further evident that there is no considerable increase in PV, while the concentration of nanoparticles was change. This is because of the fact that there is no substantial change in the solid concentration in the base mud system.

### Effect of particle concentration and temperature on yield point

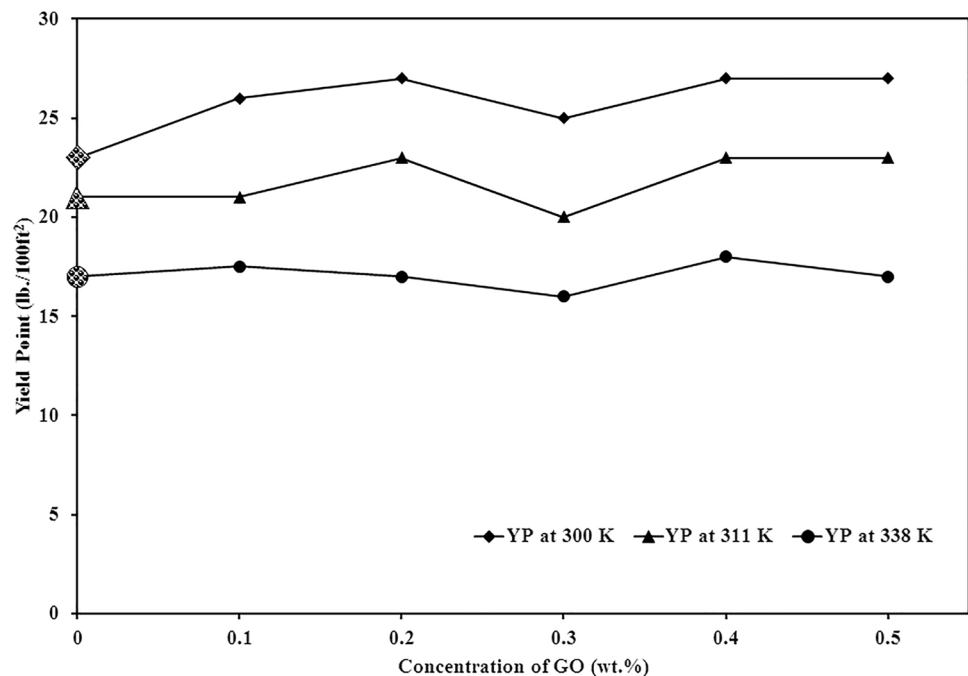
Figure 13 demonstrates the effect of changing the temperature along with nanoparticle concentration on yield point. In general, this rheological parameter is indispensable for efficient drill cutting transportation. It also exhibits the ability of the drilling fluid to remove the drill cutting from underneath the drill bit and carry it up to the surface (Ismail et al. 2016), (Ahmed et al. 2020). As there is increase in temperature, a decrease in YP was observed (Aramendiz and Imqam 2020). Moreover, a direct relationship was observed between the NPs concentration and YP, which further indicates an improve removal of cutting from the wellbore up to the surface (Ahmed et al. 2020). However, critical zone begins at temperature of 338 K in Sample 6. This is the zone where PV is greater than YP, thus, at this point, the cutting carrying capacity of the drilling fluid vanishes that ultimately leads to problems

such as high pump pressure or even packoff (Aramendiz and Imqam 2020). This problem is at a higher temperature than normal, which might be possible as a result of hydrolysis of the polymer used in the base mud (Aramendiz and Imqam 2020). However, before this point, the system works below the critical zone at all concentrations and temperatures. Furthermore, it is evident that in Sample 5, there is a reduction in YP, nevertheless, it still under the critical zone. It can be explain that at this concentration, there is less coagulation of the particles.

### Effect of particle concentration and temperature on gel strength

Gel strength is defined as the quantitative measure of the existence of electrochemical forces within drilling fluid when it is in static condition (Aramendiz and Imqam 2020). When the pumps are turned off, drilling fluid has an ability to form a gel like structure that prevents drill cutting from settling down under the action of gravity (Lalji et al. 2021c), (Aramendiz and Imqam 2020). Figure 14a–b summarizes the results of gel strength at different temperature and varying concentration of NPs. It was observe that at both 10 s and 10 min, there is a slight increase in gel strength at all three temperatures (Aramendiz and Imqam 2020). This ability of drilling fluid is considered as a positive feature as higher gel values complicate the process of cutting separation at the surface (Aramendiz and Imqam 2020). The result for both gel strength demonstrated by Sample 2 was similar to A. Aftab et al. (Aftab et al. 2017b).

**Fig. 13** Effect of temperature along with nanoparticle concentration on YP



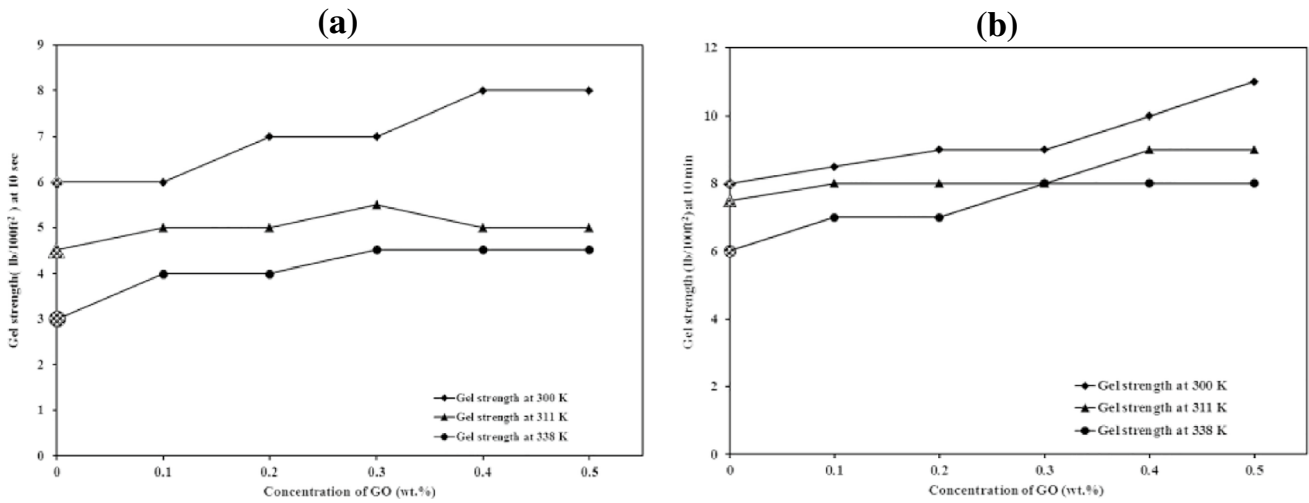


Fig. 14 Effect of temperature and nanoparticle concentration on gel strength: **a** 10 s and **b** 10 min

**Effect of particle concentration and temperature on API filter press**

Figure 15a shows the filtration volume of mud with varying concentrations of NPs. It was observed that Sample 1 resulted in 11.8 mL of filtrate volume, which reduces to 5.5 mL for the Sample 5. The smaller size of the nanoparticles improves structures and viscoelastic properties that are responsible for the reduction of fluid volume loss (Aftab et al. 2017b), (Medhi et al. 2021). Furthermore, it was perceived that there was a negative impact on filtration volume once the concentration of NPs increases beyond 0.4 wt% (Aramendiz et al. 2019). This is possible because of

the aggregation of the NPs at higher concentration, which reduces the spacing between the particles and cause high permeable filter cake (Aramendiz et al. 2019). Additionally, SEM analysis in Figure 15b was performed for the most optimized concentration of NP drilling fluid in order to evaluate the quality of the mud cake. The quality of the mud cake was analyzed based on toughness, hardness, and its durability (Lalji et al. 2021c), (Bayat et al. 2018). These factors ensure that using drilling operation wellbore integrity should be maintained by reducing filtrate volume. It was observed that the mud cake form using the NP was smooth, which can form an effective seal and controls the filtrate volume loss.

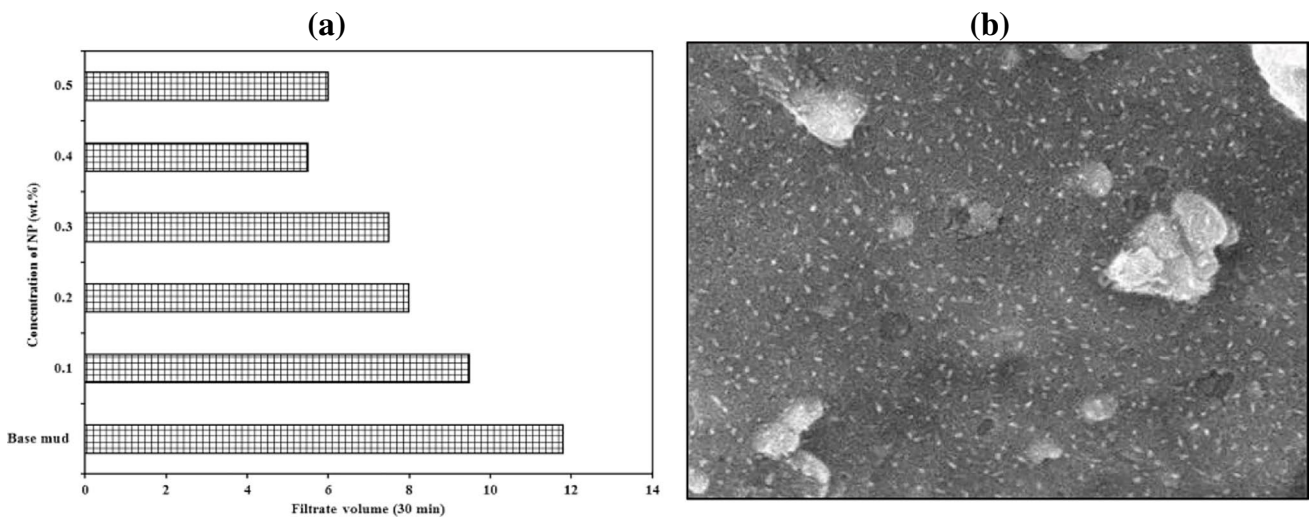


Fig. 15 Effect of NP concentration on **a** low-pressure low-temperature (LPLT) API filter press and **b** SEM analysis for Sample 5

## Effect of particle concentration on lubricity measurement

One of the most important functions of drilling fluid is to lubricate the drill bit and drill string (Ismail et al. 2016). Figure 16 illustrates coefficient of friction (CoF) for the drilling fluid in this study. It was observed that CoF slightly decrease after the addition of NP in the base mud. For the Sample 5, CoF of the drilling fluid was low, thus indicating a better performance at this concentration. It is implicit that at this concentration, a slippery layer was developed between the borehole wall and the drill string, thereby minimizing the friction. This phenomenon is interesting because the shapes of the NPs play an important role in reducing the friction between the components. A. Aftab et al. in 2016 (Aftab et al. 2017b) investigated better lubricity of the drilling mud with almost same additives. However, that study only reported lubricity at 0.1 ppb of concentration. At that concentration, the CoF reported was almost similar to 0.4 wt% concentration CoF in this study.

## Shale-fluid interaction

### Immersion test and SEM analysis

A total of 15 g of shale samples were placed in compactor to form shale pellet. These samples were then immersed in

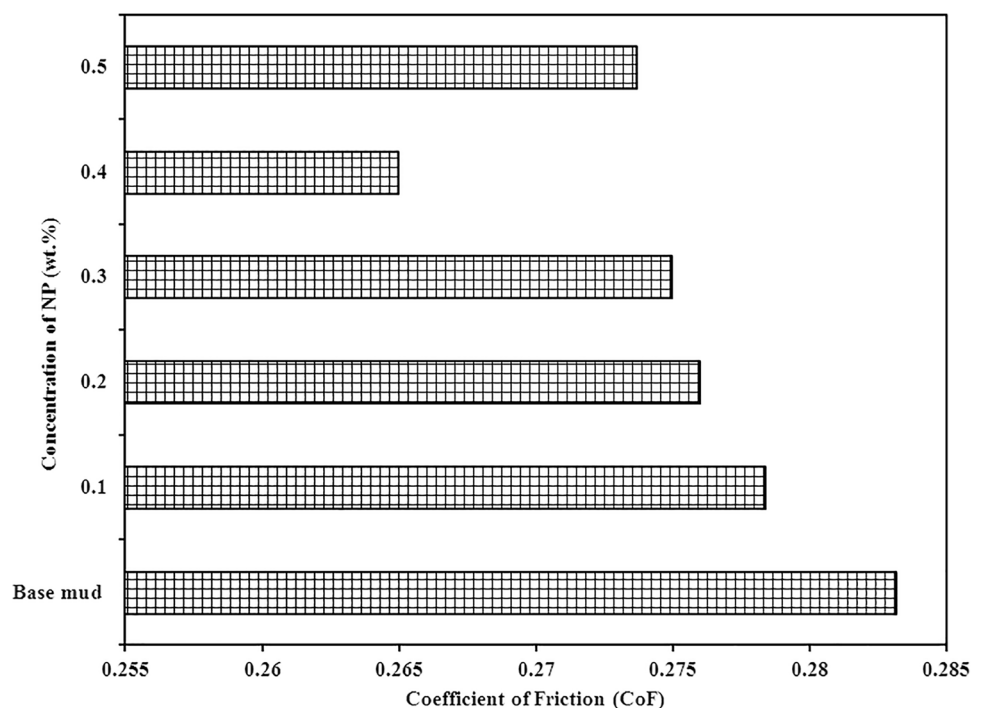
salt polymer mud and nanoparticle mud system as shown in Figure 17a and b. The samples were placed for 20 h (Aftab et al. 2017b) in order to analyze the rock fluid interaction mechanism. It was notice that in Sample 1 (Figure 17a), high erosion and cracks were observed at the boundaries of the sample. This similar behavior of the mud was also witness by A. Aftab et al. (Aftab et al. 2017b) in their study, while minimum wearing and cracks were noticed in Figure 17b when the shale was immersion in Sample 5.

Figure 18 illustrates SEM analysis of the interaction between the NP mud and the shale formation. Before the interaction as shown in Figure 5, a large number of nanospacing was observed in the shale sample. However, after the treatment with Sample 5, it was observed that the nanoparticles effectively dispersed on the surface of the shale formation, thereby covering the nanospacing in the shale. It was further noticed that a stable structure was shaped during this rock fluid interaction.

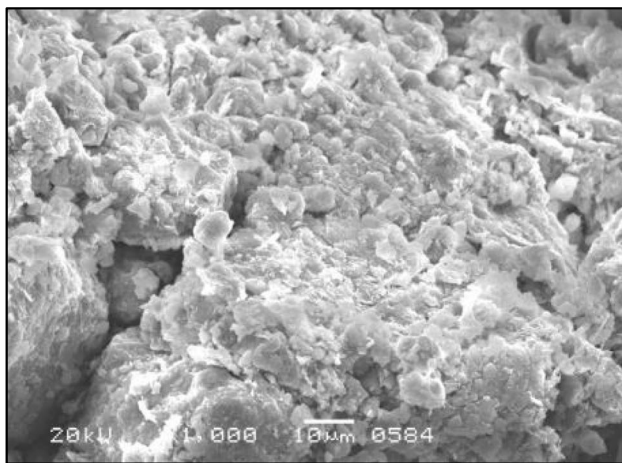
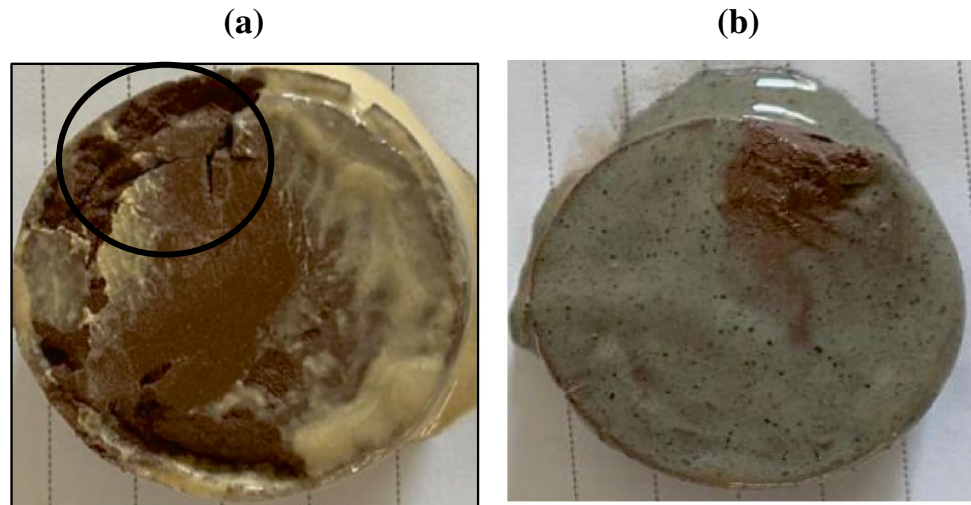
### Qualitative bulk hardness test

Table 2 depicts the qualitative hardness test of the shale sample when it comes in contact with the mud. During this test, two samples of shale that were used in the immersion test were used. On these samples, different weights were placed and qualitative hardness was evaluated. The results clearly show that the sample exposed to the salt polymer mud system was comparatively weaker than the sample

**Fig. 16** Effect of NPs concentration on lubricity



**Fig. 17** Immersion test of shale sample in **a** base mud and **b** NP mud



**Fig. 18** SEM analysis of the shale sample after immersion test

which was exposed to 0.4 wt% of NP. The sample exposed to salt polymer mud starts to crack when 6 kg of weight was placed on the sample, and it was permanently damaged on 9 kg of weight. On the other hand, NP mud sample was almost 67% stronger and was completely disintegrate on 15 kg weight.

Figure 19 represents the schematic of the interaction between the GO and montmorillonite mineral in shale formation. The active groups present in graphene oxide sheet such as hydroxyl, carboxyl, and epoxy interacts with the active functional groups of montmorillonite such as hydroxyl

through hydrogen bonding (An et al. 2018). Moreover, GO is hydrophilic in nature, hence, this part attracts the hydrophilic part of montmorillonite. This interaction makes the surface of clay mineral hydrophobic, which prevents further migration of water molecules and provides necessary stability to the formation (Rana et al. 2020), (Lv, et al. 2020). Furthermore, this communication helps nanoparticle to adsorb on the mineral surface and provide necessary hardness and strength.

**Swelling test**

Figure 20 shows the behavior of the shale sample when it was interacted with three different types of fluids, fresh water, Sample 1, and Sample 5. The samples were placed in linear dynamic swell-meter for the testing of shale swelling behavior. The shale sample used in the study comprises of 26% of clay mineral as shown in Figure 6. A total of 50% of 26% clay mineral is smectite, which demonstrates a very high swelling tendency because of large interlayer spacing and weak Vander’s Waals forces between its platelets. When the pellet of shale was exposed to fresh water, the sample demonstrates a swelling percentage of almost 20% at the end of 23 h. Moreover, the shale sample shows 11.07% of swelling in Sample 1. This system comprises of 18 g of KCL, which is acting as a shale swelling inhibitor. On the contrary, higher concentration of this compound can cause some serious environmental issues (Aftab et al. 2017).

**Table 2** Qualitative bulk hardness test of shale sample

S. no	Sample	3 kg	6 kg	9 kg	12 kg	15 kg
1	Salt polymer mud	NC	Partially broken	Broken	—	—
2	Sample 5	NC	NC	NC	Partially	Broken

NC no change

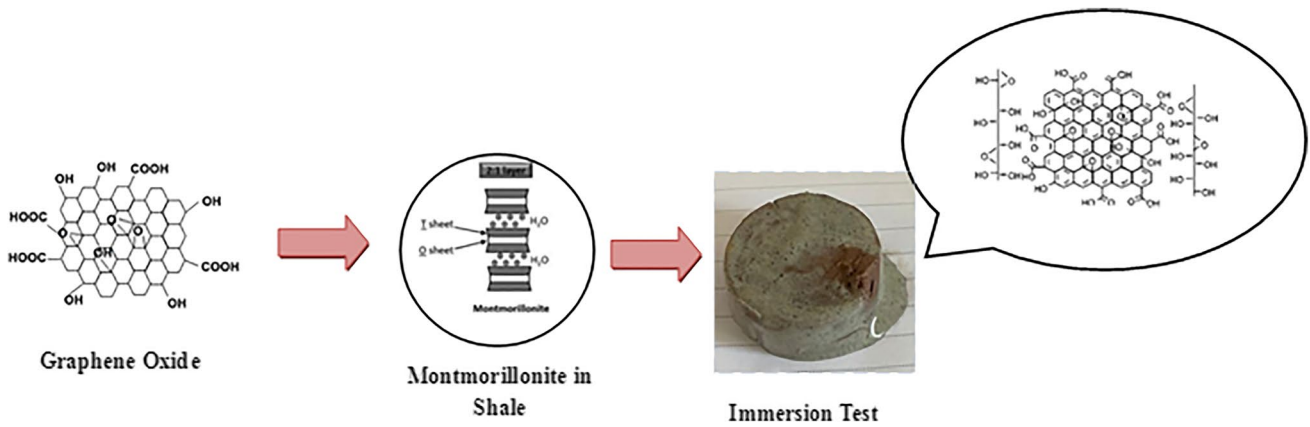
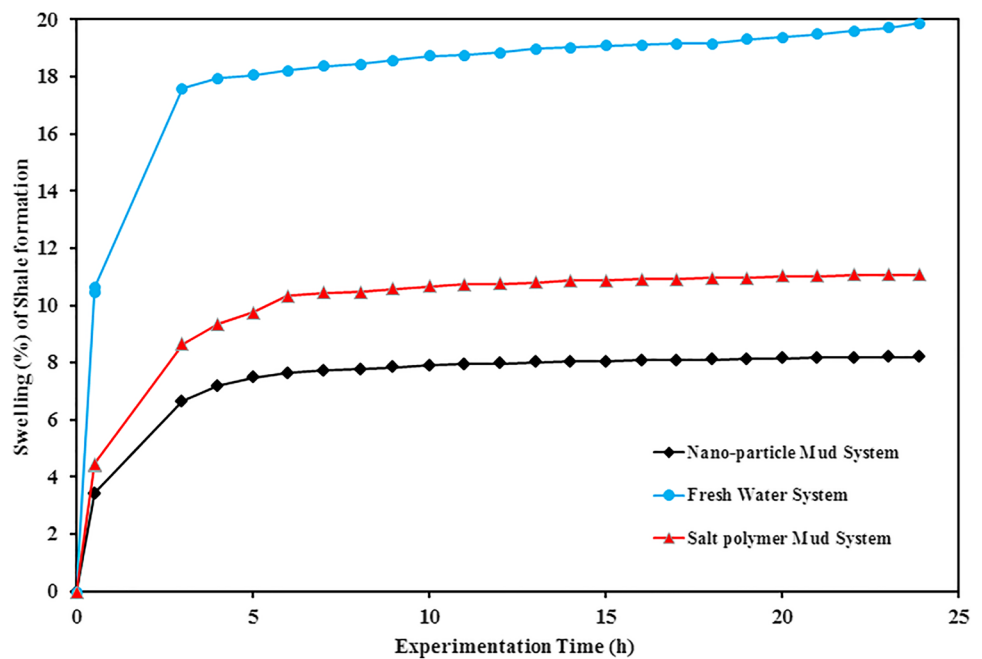


Fig. 19 Schematic of NP adhering mechanism in shale sample

Fig. 20 Swelling of shale sample using linear dynamic swell-meter



Furthermore, the swelling reduces to 8% when the sample comes in contact with Sample 5. We can conclude that the nanoparticle used in this study acts as a better clay swelling stabilizer, because it coats the shale pellet bodies and protect it from swelling and cracking.

### Conclusion

In this work, the performance of nanoparticle-based mud system was evaluated, with the purpose of creating a favorable environment of drilling shale formation. Shale stability was assessed on the basis of immersion, swelling, and bulk hardness test. It was evident from the result that when the shale sample was immersed in

nano-particle mud system, it causes less erosion and cracks onto its surface. This is due to a reason that graphene oxide nanoparticles interrelates montmorillonite present in the shale sample with the help of chemical and hydrogen bonding. This communication provides a sound stability to the shale sample and retarded the diffusion phenomenon of water molecules. In addition, improvement in rheological properties was also observed by the addition of nanoparticles in the based mud system. Moreover, the mud system with nanoparticles yields high cutting carrying capacity. This property found to be extremely useful when drilling a directional well having inclination greater than 30°, because at this inclination, cutting tends to settle down under the action of gravity if they are not properly suspended.



## Declarations

**Conflict of interest** The authors declare no competing interests.

## References

- Abdo J, Haneef MD (2011) Nano-enhanced drilling fluids: pioneering approach to overcome uncompromising drilling problems. *J Energy Resour Technol* 134(1)
- Abdo J, Haneef MD (2013) Clay nanoparticles modified drilling fluids for drilling of deep hydrocarbon wells. *Applied Clay Science* 86:76–82
- Aftab A, Ismail AR, Ibupoto ZH (2017) Enhancing the rheological properties and shale inhibition behavior of water-based mud using nanosilica, multi-walled carbon nanotube, and graphene nanoplatelet. *Egyptian Journal of Petroleum* 26(2):291–299
- Aftab A et al (2017a) Nanoparticles based drilling muds a solution to drill elevated temperature wells: a review. *Renew Sustain Energy Rev* 76:1301–1313
- Aftab A, Ismail AR, Ibupoto ZH (2017b) Enhancing the rheological properties and shale inhibition behavior of water-based mud using nanosilica, multi-walled carbon nanotube, and graphene nanoplatelet. *Egypt J Pet* 26(2):291–299
- Aftab A, et al. (2020) Environmental friendliness and high performance of multifunctional Tween 80/ZnO-nanoparticles-added water-based drilling fluid: an experimental approach. *ACS Sustain Chem Eng*
- Aftab A, et al. (2020) Influence of tailor-made TiO<sub>2</sub>/API bentonite nanocomposite on drilling mud performance: Towards enhanced drilling operations. *Appl Clay Sci* 199
- Ahmed N, Alam MS, Salam MA (2020) Experimental analysis of drilling fluid prepared by mixing iron (III) oxide nanoparticles with a KCl–Glycol–PHPA polymer-based mud used in drilling operation. *J Petrol Explor Prod Technol* 10:3389–3397
- Al-Ansari A, Parra C, Abahussain A, Abuhamed Amr M, Pino R, El Bialy M, Mohamed H, Lopez C (2017) Reservoir drill-in fluid minimizes fluid invasion and mitigates differential stuck pipe with improved production test results, in Paper presented at the SPE Middle East Oil & Gas Show and Conference, SPE, Editor. SPE: Manama, Kingdom of Bahrain.
- Ali SI, Hawkett B, Heuts JPA, van Herk AM (2009) Polymer encapsulated gibbsite nanoparticles: efficient preparation of anisotropic composite latex particles by RAFT-based starved feed emulsion polymerization. *Langmuir* 25:10523–10533
- Ali A, Faisal S, Rehman K et al (2015) Tectonic imprints of the Hazara Kashmir Syntaxis on the Northwest Himalayan fold and thrust belt North Pakistan. *Arab J Geosci* 8:9857–9876
- Ali Esfandyari Bayata PJM, Pirooziana A, Rafatib R (2018) Experimental investigation of rheological and filtration properties of waterbased drilling fluids in presence of various nanoparticles. *Colloids Surf A*, (555):256–263
- Alvi MA, Belayneh M, Saasen A, BS Aadnøy (2018) The effect of micro-sized boron nitride BN and iron trioxide Fe<sub>2</sub>O<sub>3</sub> nanoparticles on the properties of laboratory bentonite drilling fluid, in Paper presented at the SPE Norway One Day Seminar. 2018: Bergen, Norway
- Amanullah MA.-T.A. AM (2009) Nano-technology—its significance in smart fluid development for oil and gas field application. In SPE Saudi Arabia Section Technical Symposium, SPE, Editor. Society of Petroleum Engineers: Al-Khobar, Saudi Arabia. p. 1–12
- Amanullah M, Al-Tahini A M (2009) Nano-technology — its significance in smart fluid development for oil and gas field application, in *Paper presented at the SPE Saudi Arabia Section Technical Symposium*. Al-Khobar, Saudi Arabia
- Amanullah M, Al-Arfaj MK, Al-Abdullatif Z (2011) Preliminary test results of nano-based drilling fluids for oil and gas field application. In Paper presented at the SPE/IADC Drilling Conference and Exhibition. Amsterdam, The Netherlands
- An Y, Qu WJ, Yu PZ et al (2018) The assembly of a composite based on nano-sheet graphene oxide and montmorillonite. *Pet Sci* 15:366–374
- Aramendiz J, A.H. Imqam, SM. Fakher (2019) Design and evaluation of a water-based drilling fluid formulation using SiO<sub>2</sub> and graphene oxide nanoparticles for unconventional shales. in International Petroleum Technology Conference, SPE, Editor. Beijing, China
- Aramendiz J, Imqam A (2020) Silica and graphene oxide nanoparticle formulation to improve thermal stability and inhibition capabilities of water-based drilling fluid applied to woodford shale. *SPE Drill & Compl.* 35:164–179
- Azeem Rana MKA (2019) Saleh TA (2019) Advanced developments in shale inhibitors for oil production with low environmental footprints—a review. *Fuel* 247:237–249
- Bayat AE, Jalalat P, Piroozian A, Rafati R (2018) Experimental investigation of rheological and filtration properties of water-based drilling fluids in presence of various nanoparticles. *Colloids and Surfaces A: Physicochemical and Engineering Aspects* 555:256–263
- Bonini M, Barla Dabernadi D, M, Barla G. (2009) The mechanical behaviour of clay shales and implications on the design of tunnels. *Rock Mechanics and Rock Engineering* 42:361–388
- Bossart P, Ottiger R (1989) Rocks of the Murree Formation in Northern Pakistan: indicators of a descending foreland basin of late Paleocene to middle Eocene age. *Eclogae Geologicae Helveticae* 82(1):133–165
- Chang W, Leong YK (2014) Ageing and collapse of bentonite gels—effects of Li, Na K and Cs Ions. *Rheol Acta* 53:109–122
- De Paiva LB, Morales A, Diaz FRV (2008) Organoclays: properties, preparation and applications. *Appl Clay Sci* 42:8–24
- Díaz-Pérez A, Cortés-Monroy I, Roegiers JC (2007) The role of water/clay interaction in the shale characterization. *Journal of Petroleum Science and Engineering* 58(1–2):83–98
- Fink J (2015) Petroleum engineer's guide to oil field chemicals and fluids. 2nd Edition ed. Elsevier. Gulf Professional Publishing
- Gholami R et al (2018) A review on borehole instability in active shale formations: Interactions, mechanisms and inhibitors. *Earth Sci Rev* 177:2–13
- He H, Duchet J, Galy J, Gerard J-F (2005) Grafting of swelling clay materials with 3-aminopropyltriethoxysilane. *J. Colloid Interface Sci* 288(1):171–176
- Hui Mao ZQ (2015) Zhonghou Shen, Weian Huang, *Hydrophobic associated polymer based silica nanoparticles composite with core-shell structure as a filtrate reducer for drilling fluid at ultra-high temperature*. *J Petrol Sci Eng* 129:1–14
- Ismail AR, Aftab A, Ibupoto ZH, Zolkifile N (2016) The novel approach for the enhancement of rheological properties of water-based drilling fluids by using multi-walled carbon nanotube, nanosilica and glass beads. *Journal of Petroleum Science and Engineering*. 139:264–275
- Ismail AR, Rashid MSA, Thameem AB (2018) Application of nano-materials to enhanced the lubricity and rheological properties of water based drilling fluid. in IOP Conf. Series: Materials Science and Engineering. IOP Publishing
- Johnson DW, B.P.D., Karl S. (2015) Coleman, A manufacturing perspective on graphene dispersions. *Curr Opin Colloid Interface Sci* 20(5–6):367–382
- Kai Wang GJ, Li X, Luckham PF (2020) Study of graphene oxide to stabilize shale in water-based drilling fluids. *Colloids Surf A*, 606
- Khan MA, et al. (2020) Experimental study and modeling of water-based fluid imbibition process in Middle and Lower Indus Basin Formations of Pakistan. *J Petrol Explor Product Technol*

- Khodja MC, Canselier Jean Paul, Bergaya F, Fourar K, Khodja M, Cohaut N, Benmounah A (2010) Shale problems and water-based drilling fluid optimisation in the Hassi Messaoud Algerian oil field. *Applied Clay Science* 49:383–393
- Lalji SM, Ali SI, Awan ZUH et al (2021a) A novel technique for the modeling of shale swelling behavior in water-based drilling fluids. *J Petrol Explor Prod Technol* 11:3421–3435
- Lalji SM, Ali SI, Ahmed R, et al (2021b) Comparative performance analysis of different swelling kinetic models for the evaluation of shale swelling. *J Petrol Explor Prod Technol*
- Lalji SM, Khan MA, Haneef J, et al. (2021c) Nano-particles adapted drilling fluids for the swelling inhibition for the Northern region clay formation of Pakistan. *Appl Nanosci*
- Lalji SM, Ali SI, Awan ZUH, et al. (2022) Development of modified scaling swelling model for the prediction of shale swelling. *Arab J Geosci*. 15(353)
- Lv K, et al. (2020) Study of Janus amphiphilic graphene oxide as a high-performance shale inhibitor and its inhibition mechanism. *Front Chem* 8
- Mballa MAM, Heuts JPA, van Herk AM (2013) Encapsulation of non-chemically modified montmorillonite clay platelets via emulsion polymerization. *Colloid Polym Sci* 291:501–513
- Medhi S, Chowdury S, Bhatt N, Gupta DK, Rana S, Sangwai JS (2021) Analysis of high performing graphene oxide nanosheets based non-damaging drilling fluids through rheological measurements and CFD studies. *Powder Technology* 377:379–395
- Messaoudi A, Bouzit M, Boualla N (2018) Physical and rheological properties of the Chorfa dam mud: dependency on solids concentration. *Appl Water Sci* 8(178)
- Mobeen Murtaza HMA, Kamal MS, Hussain SMS, Mahmoud M, Patil S (2020) Evaluation of clay hydration and swelling inhibition using Quaternary ammonium dicationic surfactant with phenyl linker. *Molecules* 25(4333)
- Mortatha Al-Yasiri AA (2019) Shahid Pervaiz, Dongsheng Wen, *Influence of silica nanoparticles on the functionality of water-based drilling fluids*. *J Petrol Sci Eng* 179:504–512
- Moslemzadeh AS, Reza S, Moomenie M (2015) Experimental investigation of the effect of henna extract on the swelling of sodium bentonite in aqueous solution. *Appl Clay Sci* 105
- Mughal MS, Zhang C, Du D, Zhang L, Khan Mustafa S, Hameed F, Khan R, Zaheer M, Blaise D (2018) Petrography and provenance of the Early Miocene Murree Formation, Himalayan Foreland Basin, Muzaffarabad, Pakistan. *Journal of Asian Earth Sciences* 162(15):25–40
- Mughal MS, Zhang C, Du D, Zhang L, Mustafa S, Hameed F, Khan MR, Zaheer M, Blaise D (2018) Petrography and provenance of the Early Miocene Murree Formation, Himalayan Foreland Basin, Muzaffarabad, Pakistan. *Journal of Asian Earth Sciences*. 162:25–40
- Needaa Al-Malki PP, Al-Hadrami H, Abdo J (2016) Controlling bentonite-based drilling mud properties using sepiolite nanoparticles. *Petroleum Exploration and Development* 43(4):717–723
- Oort EV (2003) On the physical and chemical stability of shales. *Journal of Petroleum Science and Engineering* 38:213–235
- Rana A, Arfaj MK, Saleh TA (2020) Graphene grafted with glucopyranose as a shale swelling inhibitor in water-based drilling mud. *Appl Clay Sci*. 199:105806
- Ravi Kumar MK (2019) Anil Kumar, Rakesh Singh, Rajesh Kashyap, Sumita Rani, Dinesh Kumar, *Surface modification of graphene oxide using esterification*. *Materials Today: Proceedings* 18(3):1556–1561
- Riley M, Stamatakis E, Young S, Price Hoelscher K, De Stefano G, Ji L, Guo Q, Friedheim J (2012) *Wellbore stability in unconventional shale — the design of a nano-particle fluid*, in *Paper presented at the SPE Oil and Gas India Conference and Exhibition*. SPE
- Sadeghalvaad M, Sabbaghi S (2015) The effect of the TiO<sub>2</sub> /polyacrylamide nanocomposite on water-based drilling fluid properties. *Powder Technol* 272:113–9
- Saleh TA (2019) Ibrahim MA, Advances in functionalized nanoparticles based drilling inhibitors for oil production. *Energy Reports* 5:1293–1304
- Sengupta P, Saikia PC, Borthakur PC (2008) SEM-EDX characterization of an iron rich kaolinite clay. *J Sci Ind Res* 67:812–818
- Sharma MM, Zhang R, Chenevert ME, Ji L, Guo Q, Friedheim J (2012) A new family of nanoparticle based drilling fluids, in *Paper presented at the SPE Annual Technical Conference and Exhibition*. San Antonio, Texas, USA.
- Steiger RP, Peter K (1992) Leung, *Quantitative determination of the mechanical properties of shales*. *SPE Drill Eng* 7:181–185
- Swai RE (2020) A review of molecular dynamics simulations in the designing of effective shale inhibitors: application for drilling with water-based drilling fluids. *J Petrol Explor Prod Technol* 10:3515–3532
- Wang F, Tan X, Wang R et al (2012) High temperature and high pressure rheological properties of high-density water-based drilling fluids for deep wells. *Pet Sci* 9:354–362
- Yuxiu An GJ (2015) Yanjun Ren, Lingyu Zhang, Yourong Qi, Qingying Ge, An environmental friendly and biodegradable shale inhibitor based on chitosan quaternary ammonium salt. *J Petrol Sci Eng* 135:253–260
- Zakaria MF (2013) Nanoparticle-based drilling fluids with improved characteristics. University of Calgary, Calgary
- Zakaria M, H.M., Harland G (2012) Novel nanoparticle-based drilling fluid with improved characteristics. in *SPE International Oilfield Nanotechnology Conference and Exhibition*, S.o.P. Engineers, Editor. Society of Petroleum Engineers: Noordwijk, The Netherlands. p. 1–6
- Zakaria MF, Maen H, Hareland G (2012) Novel nanoparticle-based drilling fluid with improved characteristics, in *Paper presented at the SPE International Oilfield Nanotechnology Conference and Exhibition*. Noordwijk, The Netherlands
- Zhang H, Zhong Y, She J et al (2019) Experimental study of nano-drilling fluid based on nano temporary plugging technology and its application mechanism in shale drilling. *Appl Nanosci* 9:1637–1648
- Zhao S, Yan JN, Shu Y et al (2008) Rheological properties of oil-based drilling fluids at high temperature and high pressure. *J. Cent. South Univ. Technol.* 15:457–461